



A promising broadband and thin microwave absorber based on ternary FeNi@C@polyaniline nanocomposites

Journal:	<i>RSC Advances</i>
Manuscript ID	RA-ART-09-2015-019816.R1
Article Type:	Paper
Date Submitted by the Author:	17-Oct-2015
Complete List of Authors:	Han, Dandan; Northeast Dianli University, College of Science Xiao, Ningru; Tianjin Polytechnic University, College of Science Hu, He; Jilin University, College of Instrumentation&Electrical Engineering Liu, Bao; Northeast Dianli University, College of Science Song, Gengxin; Northeast Dianli University, College of Science Yan, He; Northeast Dianli University, College of Science
Subject area & keyword:	Nanomaterials - Materials < Materials

Cite this: DOI: 10.1039/c0xx00000x

www.rsc.org/advances

PAPER

A promising broadband and thin microwave absorber based on ternary FeNi@C@polyaniline nanocomposites

Dandan Han,^{*a} Ningru Xiao,^b He Hu,^c Bao Liu,^a Gengxin Song,^a and He Yan^a

Received (in XXX, XXX) Xth XXXXXXXXX 20XX, Accepted Xth XXXXXXXXX 20XX

DOI: 10.1039/b000000x

Ternary FeNi@C@polyaniline (PANI) nanocomposites, which FeNi@C nanocapsules are surrounded by PANI, are synthesized by combing the arc-discharge process and in-situ chemical oxidative polymerization reaction. The strong interactions between carbon shell and PANI result in the blue shift of Raman spectrum. The effect of PANI on the electromagnetic properties of FeNi@C nanocapsules is investigated at 2-18 GHz. The bandwidth (reflection loss (RL)<-10 dB) of FeNi@C@PANI nanocomposites keeps the constant of 3.0 GHz, but the frequency range (RL<-10 dB) shifts to lower frequency with increasing thickness from 1.7 to 3.0 mm. For the thickness of 1.4 mm, the bandwidth of FeNi@C@PANI nanocomposites reaches the maximum value of 5 GHz (13-18 GHz). For the FeNi@C@PANI nanocomposites, an minimum RL(RL_{min}) of -49.2 dB is observed at 16.6 GHz for the thickness of 1.3 mm. The RL_{min} of FeNi@C@PANI nanocomposites is larger than that of FeNi@C nanocapsules and the RL_{min} shifts from low to high frequency under the same absorbing thickness. The FeNi@C@PANI nanocomposite can be as good candidate for the lightweight, thin and strong absorptive microwave absorbers with broad bandwidth.

1. Introduction

With the rapid development of electronic information technology, the dominant frequency range of communication devices has shifted toward the GHz frequency range in order to enhance the data transfer rates and capacity. As a result, the electromagnetic (EM) radiation is becoming more and more dense and messy in our living space, which endangers public health and safety enormously. Therefore, studying of the EM absorption absorber, which can let the incidence EM wave incidence into the absorber and then attenuate it into thermal energy, has attracted extensive attention.¹⁻¹⁰ The EM absorption performances of absorbers are determined by EM impedance matching between complex permeability and complex permittivity.¹⁻⁴ Core-shell structured nanocapsules, which are usually composed of a core and a shell of nanometer size that are made of different materials, often exhibit improved physical and chemical properties over their single component counterpart.^{5,6} Due to the proper EM matching between magnetic cores and dielectric shells, core-shell structured nanomaterials with different materials, morphologies and geometries have been proved to be efficient in improving EM performances of materials. A high-performance microwave absorbing composite based on heterostructured nanorods with porous magnetite core and carbon shell was realized by combining a hydrothermal carbonization coating process and a controlled carbothermal reduction.⁷ Li et al reported that the effective absorption bandwidth of mesoporous Fe/C and core-shell Fe-Fe₃C@C nanocapsules reached 3.36 and 5.04 GHz with the matching thickness of 2 and 1.5 mm correspondingly.⁸ Zhao et al synthesized core-shell structured

Ni@ZnO composites with different morphology and investigated the influence of morphology on the microwave absorption abilities.⁹ Wang et al used the traditional arc discharge method to prepare the Ni@C nanocapsules and adjusted the optimal working frequency with adequate microwave absorption by varying the thickness of the C shell.¹⁰ In Liu's previous studies, the arc-discharge technique was used to uniformly synthesize different kinds of core-shell structured nanocapsules with various shell and core materials, e.g., Al₂O₃-coated FeCo nanocapsules, carbon- and ZnO-coated nanocapsules with a core consisting of a single element, an alloy or an intermetallic compound and their microwave absorption performance was systematically investigated.¹¹⁻¹⁵ However, the reported core/shell structured nanomaterials mainly exhibit strong absorptions in high-frequency bands of microwaves (10-18 GHz in the X and Ku bands) with narrow absorbing bandwidths and is sensitive with absorber thickness (>10% for a change in absorber thickness by 10%), due to the limited material-phase variety constrained by their single core/shell structure.¹⁶

In order to enhance microwave absorption performance, the preparation of organic/inorganic nanocomposites is considered as a effective way. These nanocomposites can induce beneficial physical effects on microwave absorption at an applied EM field, including reflecting and scattering inside materials, cooperative effects of dielectric and magnetic properties, and multi-polarizations at interfaces of the two components.¹⁷ The conductive organic polymers conduct electricity due to their chain-conjugated π electrons, good environmental stability and also interesting electronic properties. The polymer can act as a

matrix between the magnetic nanoparticles, which give rise to the enhanced dielectric loss and good impedance match. It also reduces the density of magnetic nanoparticles realizing the demand of microwave absorbers with high-efficiency absorption and low-density.¹⁸ Among the large family of conductive polymers, polyaniline (PANI) is a remarkable polymer which possesses great advantages, such as excellent environmental stability and high levels of EM shielding performances at microwave frequencies.¹⁹⁻²⁵ Various PANI-based materials and magnetic nanoparticles have been combined by wet chemical method to improve the EM absorption, such as Ni@PANI nanocapsules, Fe₃O₄@PANI nanocapsules, ultrasmall Ni/PANI nanocomposites, Ni_{0.5}Zn_{0.5}Fe₂O₄@PANI nanostructures, nickel/ferrite/PANI composites and reduced graphene oxide/flake carbonyl iron powders/PANI composites.²⁶⁻³¹ However, in these nanocomposites, the magnetic nanoparticles may be easily destroyed by acid solution.

The core/shell structure with carbon shell display a strong anti-acid effect and can protect the magnetic core.³² Core/shell/shell-structured Ni/C/PANI nanocapsules were prepared and their microwave absorbing properties were evaluated in the 2-18 GHz. A 3 mm-thick paraffin-bonded nanocapsules absorber shows an extremely broad -5 dB-bandwidth of 3.4-18 GHz in almost the whole S-Ku bands.¹⁶ The double-shelled Co/C/PANI nanocomposites were prepared by combing the arc-discharge process and in-situ chemical oxidative polymerization reaction. Reflection loss (RL) exceeding -10 dB is obtained in 9.9-16.4 GHz for the absorber thickness of 2.5 mm, which cover almost half of X-band (8-12 GHz) and most of Ku-band (12-18 GHz).¹⁷ However, the EM absorption strength of Ni/C/PANI and Co/C/PANI nanocapsules is too low to meet actual needs. The weak absorption strength of Ni/C/PANI and Co/C/PANI nanocapsules can be attributed to the low concentration of Ni@C and Co@C nanoparticles and the weak EM absorption performance of Ni@C and Co@C nanoparticles. Liu et al reported the synthesis of FeNi@C by the arc discharge method and investigated its EM properties. For the thickness of 2.0 mm, RL exceeding -10 dB was obtained in the whole Ku-band, while it exceeds -20 dB over the 13.6-16.6 GHz range and an optimal RL of -26.9 dB was observed at 16 GHz.¹¹ Therefore, the synthesis of FeNi@C@polyaniline nanocomposites is imperative if it is to be used as the broadband, lightweight, thin and strong absorbing microwave absorber.

In this paper, we report the synthesis of ternary FeNi@C@PANI nanocomposite, which FeNi@C core-shell structured nanocapsules are doped in PANI. In this way, not only the strong EM absorption can be varied but also the dielectric properties of the nanocapsules can be optimized in order to improve the impedance match, to broaden the EM wave absorption bandwidth and to enhance the absorption.

2. Experimental

2.1 Materials

Iron and nickel bulk, ethanol, HCl, 4-aminobenzoic acid (ABA), aniline, ammonium peroxodisulfate (APS) were obtained from Jilin Chemical Company (Jilin, China). All chemicals were of analytical grade and used without further purification. Distilled

water was used in all experiments.

2.2 Synthesis of FeNi@C nanocapsules

FeNi@C nanocapsules were prepared by the modified arc-discharge method described in detail elsewhere.¹⁰⁻¹⁷ In brief, bulk FeNi alloy on a water-cooled copper crucible was used as the anode. The cathode was a carbon needle. After the chamber was evacuated, 1.6×10^4 Pa of pure argon and 0.4×10^4 Pa of hydrogen and 40 ml liquid ethanol were introduced into the chamber. The arc discharge current was maintained at 100 A for 0.5 h. Then the products were collected from depositions on the top of the water-cooled chamber, after passivated for 24 h in air.

2.3 Preparation of FeNi@C@PANI nanocomposites

FeNi@C@PANI nanocomposites were prepared by a chemical polymerization process. Firstly, to remove the oxide impurity in the FeNi@C nanocapsules, the as-prepared FeNi@C nanocapsules were dispersed into 0.1 mol/L HCl aqueous solution under ultrasonic vibrations for 30 min. Afterward, the FeNi@C nanocapsules with hydroxyl on its surface were modified by a chemical graft procedure and prepared in a 0.1 mol/L ABA alcohol solution under stirring at 50 °C for 1 h. Finally, the resultant ABA-grafted FeNi@C nanocapsules were dispersed into a pH=2 HCl aqueous solution of aniline (0.50 mol/L) under ultrasonic vibrations for 1 h. Then, a 1 mol/L aqueous solution of APS was drop added into the dispersoid for 2 h under stirring at 0 °C. The mixture was further stirred for 4 h, in which a chemical oxidative polymerization of aniline was carried out to obtain HCl-protonated PANI. In this process, a polymerization reaction between the grafted amine of ABA and aniline occurred. The product was filtered by magnetic field separation and washed with de-ionized water several times, and then dried at 60 °C for 24 h.

2.3 Materials characterizations

The phase purity of the products was characterized by X-ray powder diffraction (XRD) using Bruker D8 Advance automated X-ray diffractometer system with Cu-K α radiation ($\lambda=1.5418$ Å). The morphology, microstructure and the size distribution of the products were determined by transmission electron microscopy (TEM, JEOL-2010). Raman spectra were recorded using a micro-Raman spectrometer (Witech CRM200, the excitation wavelength at 532 nm). The measurements of EM parameters for the specimens were carried out using vector network analyzer (Anritsu 37269D) in the 2-18 GHz ranges. The samples were prepared by dispersing the FeNi@C nanocapsules and FeNi@C@PANI nanocomposites powders in paraffin (microwave transparent binder), respectively. The weight fraction of the powders is 40 %. The powder/paraffin composites were pressed to form cylindrical toroidal specimens with 7.00 mm outer diameter, 3.04 mm inner diameter, and 2 mm thickness.

3. Results and Discussion

The XRD patterns of FeNi@C nanocapsules and FeNi@C@PANI nanocomposites are shown in Fig.1. As can be seen, for FeNi@C nanocapsules, there exist three main diffraction peaks at 43.9°, 51.2°, and 75.4° corresponded to the crystalline

planes of (111), (200) and (220), indicating the presence of FeNi. In the previous report, no reflection for oxides and carbides were found in XRD pattern.^{5,10-16} In the present experiment, the same phenomenon is also observed, due to the protection from carbon shell during the arc discharge process. In addition, due to the breaking down of the translation symmetry along radial direction, no pure carbon peak can be detected, which is consistent with previous reports. While for the FeNi@C@PANI nanocomposite, apart from the characteristic peaks of FeNi, there are also one weak and broad diffraction peak in around 25°, which are assigned to the scattering from periodicity perpendicular PANI chain.³³ The XRD results reveal the co-existence of FeNi@C and PANI in the FeNi@C@PANI nanocomposites.

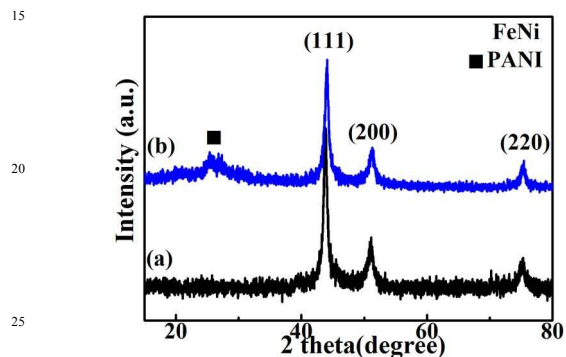


Fig. 1. XRD spectra of (a) FeNi@C nanocapsules and (b) FeNi@C@PANI nanocomposites.

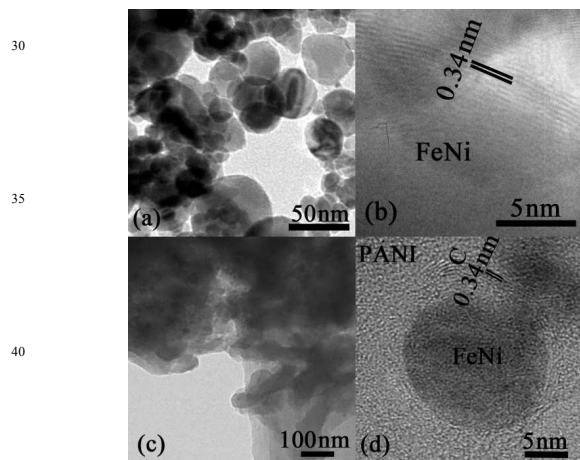


Fig. 2. (a) TEM and (b) HRTEM images of FeNi@C nanocapsules; and (c) TEM and (d) HRTEM images of FeNi@C@PANI nanocomposites.

To investigate the microstructure and morphology of FeNi@C nanocapsules and FeNi@C@PANI nanocomposites, TEM and HRTEM studies have been made. A representative overview of the TEM image in Fig.2(a) confirms the spherical shape of the FeNi@C nanocapsules with some irregular spheres. The measured diameter ranges from 10 to 70 nm. The detailed microstructure of shell of FeNi@C nanocapsules is shown in the HRTEM images (Fig.2(b)). One can see that the FeNi@C have the core-shell structure and the shell has a good layered structure with a distance between the layers of about 0.34 nm, which

agrees with the interplanar spacing of the (002) plane of graphite. After the in-situ oxidative polymerization reaction, TEM image in Fig. 2(c) indicates that the FeNi@C nanocapsules were surrounded by PANI. The HRTEM image in Fig.2(d) shows that the FeNi@C nanocapsules still retain their original core-shell structure, which proves the carbon shell can protect magnetic nanoparticles from the HCl.

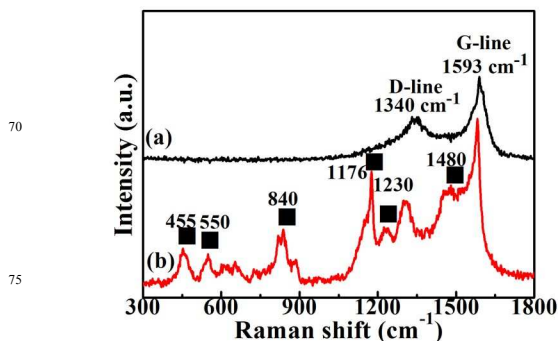


Fig. 3. Raman spectra of (a) FeNi@C nanocapsules and FeNi@C@PANI nanocomposites.

Raman spectroscopy can be used to measure the vibrational spectra of nonpolar bonds such as crystal-lattice vibrations and carbon-carbon bonds.³⁴ To further study the interaction between these FeNi@C nanocapsules and PANI, Raman spectroscopy analysis is employed. As shown in Fig.3, the spectra are collected within the range between 300 and 1800 cm⁻¹. For FeNi@C nanocapsules, the Raman spectrum (Fig.3(a)) displays the so-called D peak at 1340 cm⁻¹, which can be related to the presence of disorder in the graphite lattice, and G peak at 1593 cm⁻¹, indicative of the amount of perfectly crystalline graphite.³⁴ For the Raman spectrum of FeNi@C@PANI nanocomposites shown in Fig.3(b), the out-of-plane C-H wag, out-of-plane C-N-C torsion, imine deformation, in-plane C-H bending, in-plane ring deformation, and C=N stretching of quinoid are situated at 455, 550, 840, 1176, 1230 and 1480 and 1593 cm⁻¹, respectively.³⁵ Compared with FeNi@C nanocapsules, two characteristic peaks (1305 and 1583 cm⁻¹) originating from the carbon structure in FeNi@C@PANI exhibit the clear blue shift. The bands at 1305 and 1583 cm⁻¹ correspond to C-N⁺ stretching and C-C stretching of benzoid, respectively.³⁶ The strong interactions between carbon shell and PANI result in the blue shift.

To evaluate microwave absorption performance of the products, the FeNi@C@PANI nanocomposites (40 wt%) were mixed with paraffin uniformly and then pressed into a cylindrical model with thickness of 2.00 mm. The relative complex permittivity ($\epsilon_r = \epsilon' - j\epsilon''$) and permeability ($\mu_r = \mu' - j\mu''$) of FeNi@C@PANI nanocomposites were measured with a vector network analyzer in the 2-18 GHz range. For the purpose of comparison, the EM parameters of FeNi@C nanocapsules were also investigated under the same conditions. The real permittivity (ϵ') and real permeability (μ') symbolize the storage ability of electric and magnetic energy, while the imaginary permittivity (ϵ'') and imaginary permeability (μ'') are related to the dissipation of electric and magnetic energy.³⁷ For both samples, the downtrend was observed on the ϵ' and ϵ'' curves, due to increased lagging behind of the dipole-polarization response with respect to the electric-field change at

GHz frequency range.¹⁰

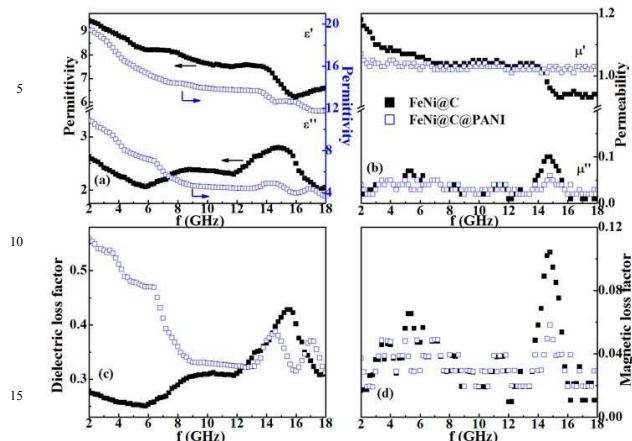


Fig. 4. Frequency dependence of (a) relative complex permittivity, (b) relative complex permeability, (c) dielectric loss factor and (d) magnetic loss factor of paraffin-bonded composites with FeNi@C nanocapsules and FeNi@C@PANI nanocomposites.

It is found that some slight peaks existed on the ϵ' and ϵ'' parts of ϵ_r , which are possibly depends on ionic, electronic, orientational and space charge polarization.¹⁷ Among the polarization mechanisms, space charge polarization (interfacial polarization) is more frequency-dependent. According to Maxwell-Wagner polarization theory, the accumulation of space charges at the interface of two media will lead to interfacial polarization in a heterogeneous system.³⁸ Compared with FeNi@C nanocapsules, the additional interface between carbon shells and PANI contribute to the extra slight peak in FeNi@C@PANI nanocomposites.³⁹ In addition, it is clear observed that the ϵ' and ϵ'' of FeNi@C@PANI nanocomposites is larger than that of FeNi@C nanocapsules, respectively. The ϵ' is mainly associated with the amount of polarization occurring in the material. Compared with FeNi@C nanocapsules, the introduction of PANI can increase the amount of polarization.¹⁷ On the basis of Debye theory on dielectric, ϵ'' is generally known as $\epsilon'' = \omega\tau(\epsilon_S - \epsilon_\infty)/(1 + \omega^2\tau^2) + \sigma/\omega\epsilon_0$, where ϵ_S is the static permittivity, ϵ_∞ the relative dielectric permittivity at the high-frequency limit, ω the angular frequency, τ the polarization relaxation time, and σ the electrical conductivity. Because ϵ_S , ϵ_∞ , ω and τ are the intrinsic parameters of materials, σ is the key factor of determining the ϵ'' .⁴⁰ In the FeNi@C nanocapsules, it is already well documented that electrical conductivity of nanocapsules is mainly from the onion-like carbon shells. With respect to the micro-composites, the nano-sized metallic particles in nanocapsules are weak on the metallic behavior and the electrical conductivity is reduced by the disorder atoms on the surface of nanoparticles.⁴¹ In the FeNi@C@PANI nanocomposites, the PANI would increase the contact area of FeNi@C nanocapsules and build the conducting network, in which electrons can freely transfer, because of the fact that PANI is the conducting polymer and possesses lower electrical resistance than onion-like carbon shells. Therefore, the induction of PANI can increase the value of ϵ'' , which is significant for the enhanced EM absorption abilities.

Fig. 4(b) shows the frequency dependence of the real (μ') and

the imaginary (μ'') parts of μ_r of both composites as a function of frequency in the range of 2-18 GHz. It is seen that μ' of FeNi@C@PANI nanocomposites is almost constant in the 2-18 GHz range with values of 1.04 ± 0.02 . The value of μ' of FeNi@C nanocapsules is larger than that of FeNi@C@PANI nanocomposites at 2-14.4 GHz and then it decreases rapidly with increasing the frequency, which is similar with the previous (Fe, Ni)/C nanocapsules. A decrease might be expected, in magnetic metal: on increasing frequency, eddy currents start shielding the magnetic metal, thus reducing its permeability to 0 (at infinite frequency).⁴² Meanwhile, as the frequency is varied, μ'' of two samples display a similar tendency with the multi-resonance phenomenon in the whole frequency range and exhibit the strong peak at 14.8 GHz. The first resonance peak around 5.4 GHz can be attributed to the Kittel natural resonance, which depend strongly on the effective anisotropy field, on the magnetic particle size, on the particle geometry, and no the dipole interaction between the particles.⁴³ The resonance frequency in the bulk magnetic materials usually lies in MHz frequency range. For nanoparticles, the effective anisotropy field remarkably increased due to the surface anisotropic field affected by the very-small-size effect (especially on nanoscale), which leads to the resonance frequency of nanoparticles shift to GHz frequency range.⁴⁴ The exchange-resonance mode is commonly used to explain multi-resonance behavior in small magnetic particles.⁴³ The resonance peaks around 7.0 and 14.8 GHz should be attributed to exchange-resonance modes. The small amplitude of μ'' in the FeNi@C@PANI nanocomposite should be attributed to the low magnetization of FeNi@C@PANI nanocomposites.

Fig. 4(c) and Fig. 4 (d) show the frequency dependence of the dielectric loss factor ($\tan\delta_E = \epsilon''/\epsilon'$) and magnetic loss factor ($\tan\delta_M = \mu''/\mu'$) of paraffin-bonded composites. The value of $\tan\delta_E$ in FeNi@C@PANI nanocomposites is higher than that in FeNi@C nanocapsules at 2-12.6 GHz, which is ascribed to the existence of PANI. The $\tan\delta_E$ in FeNi@C nanocapsules exhibits the big peak at 15.4 GHz, while the $\tan\delta_E$ in FeNi@C@PANI nanocomposites displays two peaks in the vicinity of 14.8 GHz and 16.8 GHz. The extra peak of FeNi@C@PANI nanocomposites may originate from the interface between carbon shell and PANI. The similar phenomena also have been observed in Au-Fe₃O₄ nanocomposites and CoNi@C nanocapsules.^{3,43} Except the peak intensity at 14.8 GHz, the $\tan\delta_M$ of both samples display a similar tendency in the whole frequency range.

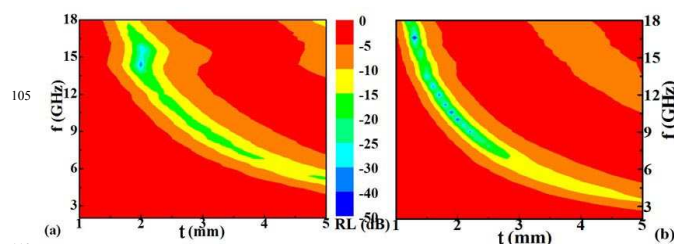


Fig. 5. Contour maps of the frequency dependence of the RL of paraffin-bonded composites with (a) FeNi@C nanocapsules and (b) FeNi@C@PANI nanocomposites as a function of the absorber thickness

The EM reflection property of a material is typically

characterized in terms of the power reflection of a plane wave reflected from an infinite slab of the material that is backed by a metallic surface.⁴⁵ The reflectivity or return loss of composites, generally produced for normal incidence, is expressed in decibels

RL(dB) as

$$RL = 20 \lg |(Z_{in} - Z_0) / (Z_{in} + Z_0)| \quad (1)$$

and

$$Z_{in} / Z_0 = \sqrt{\mu_r / \epsilon_r} \tanh(j2\pi ft \sqrt{\mu_r \epsilon_r} / c) \quad (2)$$

where Z_{in} is the impedance of the composites backed by the ground plane, Z_0 is the intrinsic impedance of free space, c is the velocity of light in free space, t is the thickness of composite, f is the frequency of the incident EM wave.

As shown in Fig. 5, the dependence of the RL of the nanocapsules/nanocomposite-paraffin composites with varying layer thickness (1.0-5.0 mm) in the 2-18 GHz ranges is presented in a two-dimensional (2D) contour plot. It can be observed that the thickness of the composites has a great influence on the microwave absorption properties, and minimum RL (RL_{min}), corresponding to the minimum absorption, gradually appeared at different frequencies. For FeNi@C nanocapsules, the results indicate that a thinner absorber layer has a wider frequency bandwidth ($RL < -10$ dB), which is consistent with the CoNi@C nanocapsules and the reported FeNi@C nanocapsules.^{11, 43} For a layer thickness of 5.0 mm, the bandwidth is 1.2 GHz (4.6-5.8 GHz). With decreasing layer thickness, the bandwidth gradually increases. In the vicinity of 2.0 mm, the bandwidth reaches a value of 5.5 GHz (12.5-18 GHz). It is worthy noted that the bandwidth of FeNi@C@PANI nanocomposites keep the constant of 3.0 GHz, but the frequency range ($RL < -10$ dB) shifts to lower frequency with increasing thickness from 1.7 to 3.0 mm. For the thickness of 1.4 mm, the bandwidth of FeNi@C@PANI nanocomposites reaches the maximum value of 5 GHz (13-18 GHz). Compared with the value of FeNi@C nanocapsules, the maximum bandwidth of FeNi@C@PANI decreases about 9%, but the thickness corresponding to the maximum bandwidth is 70% of that of FeNi@C nanocapsules. In addition, the dark blue area (-40 dB $< RL < -50$ dB) can be only observed in FeNi@C@PANI nanocomposites, indicating that FeNi@C@PANI nanocomposites possess the high absorption abilities. Thus, FeNi@C@PANI nanocomposites may be qualified to be interesting for future application as the broadband, thin and strong EM absorbing materials.

Fig.6 shows the calculated RL of wax-bonded composites containing 40 wt.% of FeNi@C nanocapsules and FeNi@C@PANI nanocomposite with selected thickness. When the thickness of absorber is 2.0 mm, the optimal RL of FeNi@C nanocapsules reaches -32.9 dB at 14.4 GHz, which is similar with the reported FeNi@C nanocapsules.¹¹ For the FeNi@C@PANI nanocomposites, an optimal RL of -49.2 dB is observed at 16.6 GHz for the thickness of 1.3 mm. The RL_{min} of FeNi@C@PANI nanocomposites is larger than that of FeNi@C nanocapsules at the same thickness, which is clearly seen in Fig.6(c). As shown in Fig.6(d), the RL_{min} shifts from low to high frequency under the same absorbing thickness, which is attributed to the shift of matching range of magnetic and dielectric loss from FeNi@C nanocapsules to FeNi@C@PANI nanocomposites. The results above demonstrate that FeNi@C@PANI nanocomposites-based

absorbent not only has strong absorption characteristic and wide absorption frequency but also is thin.

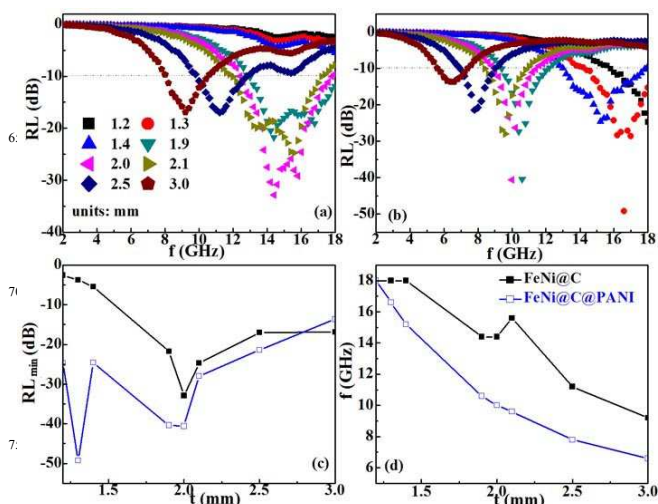


Fig.6. Frequency dependence of the microwave RL of (a) FeNi@C-paraffin composites and (b) FeNi@C@PANI-paraffin composites with the selected thickness. (c) The minimum value of RL and (d) the corresponding frequency of FeNi@C-paraffin and FeNi@C@PANI-paraffin composites at the different thickness.

In general, the thickness of absorber, absorption bandwidth, and absorption intensity are used to evaluate the absorbers in the engineering applications. The light absorbers also need to be exploited to adapt to high-speed developing nanoscience and nanotechnology. The RL_{min} , the thickness of absorber (t) corresponding to RL_{min} , and absorption bandwidth (< -10 dB) of some typical nanocomposites have been listed in Table I. In Table I, the absorbing performance of the present FeNi@C@PANI nanocomposites is compared with other nanocomposite systems reported recently. It can be seen that the FeNi@C@PANI nanocomposites have stronger RL absorption and broader bandwidth for a smaller absorber thickness. Compared with FeNi@C nanocapsules, the weight of FeNi@C@PANI nanocomposites decreases about 14.6% at the same volume. Because the density of PANI is lower than that of transition metal, the introduction of PANI can be helpful for reducing the weight of FeNi@C-based microwave absorber. The results indicate that the FeNi@C@PANI nanocomposite can be as good candidate for the lightweight, thin and strong absorptive microwave absorbents with broad bandwidth.

The excellent microwave absorption performances can be explained in the following manner. First, the FeNi-C and C-PANI interfaces are advantageous for microwave absorption due to multi-interfacial polarizations. Second, PANI can provide a greater number of active sites for microwave reflection and scattering. The microwave will be reflected and absorbed repeatedly inside the nanocomposites before being absorbed and transferred to heat. Third, the defects at the interfaces can effectively interrupt the spread of EM waves and generate dissipation due to existing impedance differences and enhance microwave absorption properties.¹⁷

Table I. Reported microwave absorption performance of some typical nanocomposites.

Sample	Weight fraction (wt.%)	RL_{min} (dB)	d (mm)	Bandwidth (<-10 dB) (GHz)	Ref.
FeNi@C	40	-26.9	2.0	5.6 (12.4-18)	11
Ni@C	40	-32	2.0	4.3(11.2-15.5)	46
Ni@ZnO	40	-46.9	2.5	8 (10-18)	14
Ni@PANI	40	-35	5.0	1.5 (16.5-18)	26
Ni@P	40	-39.9	1.7	0.55 (6.5-7.05)	47
FeCo/Al ₂ O ₃	40	-44.8	3	3 (13-16)	13
CoNi@C	40	-35	2	6 (12-18)	43
Ni@Graphene	50	-23.3	3	1.8 (11.4-13.2)	48
Ni@C@PANI	40	-9.3	3	/	16
Co/C/PANI	50	-48	7	2 (3-5)	17
FeNi@C@PANI	40	-49.2	1.3	5 (13-18)	This work

Conclusions

FeNi@C@PANI nanocomposites, which FeNi@C nanocapsules are surrounded by PANI, have been synthesized by combing the arc-discharge process and the in-situ chemical polymerization reaction. The strong interaction between carbon shell and PANI has been proved by the results of TEM and Raman. The introduction of PANI can enhance the real part and imagery part of complex permittivity. Compared with FeNi@C nanocapsules, the extra peak of FeNi@C@PANI nanocomposites in the dielectric loss may originate from the interface between carbon shell and PANI. The magnetic loss of both samples display a similar tendency in the whole frequency range. The bandwidth (RL<-10 dB) of FeNi@C@PANI nanocomposites keep the constant of 3.0 GHz, but the frequency range (RL<-10 dB) shifts to lower frequency with increasing thickness from 1.7 to 3.0 mm. For the thickness of 1.4 mm, the bandwidth of FeNi@C@PANI nanocomposites reaches the maximum value of 5 GHz (13-18 GHz). Compared with the value of FeNi@C nanocapsules, the maximum bandwidth of FeNi@C@PANI decreases about 9%, but the thickness corresponding to the maximum bandwidth is 70% of that of FeNi@C nanocapsules. For the FeNi@C@PANI nanocomposites, an optimal RL of -49.2 dB is observed at 16.6 GHz for the thickness of 1.3 mm. The RL_{min} of FeNi@C@PANI nanocomposites is larger than that of FeNi@C nanocapsules and the RL_{min} shifts from low to high frequency under the same absorbing thickness. Compared with FeNi@C nanocapsules, the weight of FeNi@C@PANI nanocomposites decreases about 14.6% at the same volume. The results indicate that the FeNi@C@PANI nanocomposite can be as good candidate for the lightweight, thin and strong absorptive microwave absorbents with broad bandwidth.

Acknowledgements

This study has been supported by the National Natural Science Foundation of China (Grant No. 11304034), and the Starting Research Fund for the Doctors of Northeast Dianli University (Grant No. BSJXM-201429).

Notes and references

- ^aCollege of Science, Northeast Dianli University, Jilin 132012, PR China. Fax/Tel: +86 432 64806631; E-mail: loveh_andan@163.com
- ^bCollege of Science, Tianjin Polytechnic University, Tianjin, 300387, PR China.
- ^cCollege of Instrumentation & Electrical Engineering, Jilin University, 130021, PR China.
- † Electronic Supplementary Information (ESI) available: See DOI: 10.1039/b000000x/
- A. Ohlan, K. Singh, A. Chandra and S.K. Dhawan, ACS Appl. Mater. Interf. 2010, 2, 927-933.
 - X.L. Wang, X.P. Liao, W.H. Zhang and B. Shi, Phys. Chem. Chem. Phys. 2015, 17, 2113-2120.
 - X.F. Zhang, P.F. Guan and J.J. Guo, Part. Part. Syst. Charact. 2013, 30, 842-846.
 - S.H. Hosseini and A. Asadnia, Inter. J. Phys. Sci. 2013, 8, 1209-1217.
 - X.G. Liu, D.Y. Geng, X.L. Wang, S. Ma, H. Wang, D. Li, B.Q. Li, W. Liu and Z.D. Zhang, Chem. Commun. 2010, 46, 6956-6958.
 - L.Y. Zhang and Z.W. Li, J. Alloys Compd. 200, 469, 422-426.
 - M. Jazirehpour and S.A. Seyyed Ebrahimi, J. Alloys. Compd. 2015, 639, 280-288.
 - G.M. Li, L.C. Wang, W.X. Li and Y. Xu, Micropor. Mesopor. Mat. 2015, 211, 97-104.
 - B. Zhao, G. Shao, B.B. Fan, W.H. Guo, Y.J. Xie and R. Zhang, J. Magn. Magn. Mater. 2015, 382, 78-83.
 - H. Wang, H.H. Guo, Y.Y. Dai, D.Y. Geng, Z. Han, D. Li, T. Yang, S. Ma, W. Liu and Z.D. Zhang, Appl. Phys. Lett. 2012, 101, 083116.
 - X.G. Liu, B. Li, D.Y. Geng, W.B. Cui, F. Yang, Z.G. Xie, D.J. Kang and Z.D. Zhang, Carbon 2009, 47, 470-474.
 - X.G. Liu, Z.Q. Ou, D.Y. Geng, Z. Han, Z.G. Xie and Z.D. Zhang, J. Phys. D: Appl. Phys. 2009, 42, 155004.
 - X.G. Liu, D.Y. Geng, S. Ma, H. Meng, M. Tong, D.J. Kang and Z.D. Zhang, J. Appl. Phys. 2008, 104, 064319.
 - X.G. Liu, J.J. Jiang, D.Y. Geng, B.Q. Li, Z. Han, W. Liu and Z.D. Zhang, Appl. Phys. Lett. 2009, 94, 053119.
 - X.G. Liu, D.Y. Geng, C.J. Choi, J.C. Kim and Z.D. Zhang, J. Nanopart. Res. 2009, 11, 2097-2104.
 - X.G. Liu, S.W. Or, C.M. Leung and S.L. Ho, J. Appl. Phys. 2014, 115, 17A507.
 - L.W. Jiang, Z.H. Wang, D. Li, D.Y. Geng, Y. Wang, J. An, J. He, W. Liu and Z.D. Zhang, RSC Adv. 2015, 5, 40384-40392.
 - Y. Xu, J.H. Luo, W. Yao, J.G. Xu and T. Li, J. Alloys Compd. 2015, 636, 310-316.
 - J. Zhao, J.P. Lin, J.P. Xiao and H.L. Fan, RSC Adv. 2015, 5, 19345-19352.
 - H.X. Jing, Q.L. Li, Y. Ye, Z.W. Guo and X.F. Yang, J. Magn. Magn. Mater. 2013, 332, 10-14.
 - H. Qiu, S.H. Qi, D.H. Wang, J. Wang and X.M. Wu, Synthetic Met. 2010, 160, 1179-1183.
 - C.L. Yuan, Y.S. Hong and C.H. Lin, J. Magn. Magn. Mater. 2011, 323, 1851-1854.
 - B. Belaabed, J.L. Wojkiewicz, S. Lamouri, N.E. Kamchi and T. Lasri, J. Alloys Compd. 2012, 527, 137-144.
 - D.G. Li, C. Chen, W. Rao, W.H. Lu and Y. H. Xiong, J. Mater. Sci: Mater. Electron. 2014, 25, 76-81.
 - C.H. Yang, J.J. Du, Q. Peng, R.R. Qiao, W. Chen, C.L. Xu, Z.G. Shuai and M.Y. Gao, J. Phys. Chem. B 2009, 113, 5052-5058.
 - X.L. Dong, X.F. Zhang, H. Huang and F. Zuo, Appl. Phys. Lett. 2008, 92, 013127.
 - Y.P. Sun, F. Xiao, X.G. Liu, C. Feng and C.G. Jin, RSC Adv. 3, 2013, 22554-22559.
 - D.D. Han, N.R. Xiao, H. Hu, B. Liu, G.X. Song and H. Yan, RSC Adv. 5, 2015, 66667-66673.
 - C.P. Wang, C.H. Li, H. Bi, J.C. Li, H. Zhang, A.J. Xie and Y.H. Shen, J.

- Nanopart. Res. 16, 2014, 2289.
- 30 B.W. Li, Y. Shen, Z. X. Yue and C.W. Nan, Enhanced microwave absorption in nickel/hexagonal-ferrite/polymer composites, *Appl. Phys. Lett.* 2006, 89, 132504.
- 31 Y. Xu, J.H. Luo, W. Yao, J.G. Xu and T. Li, *J. Alloys Compd.* 636,2015,310-316.
- 32 S. Ma, P.Z. Si, Y. Zhang, B. Wu, Y.B. Li, J.J. Liu, W.J. Feng, X.L. Ma and Z.D. Zhang, *Scripta Mater.* 57, 2007, 265-268.
- 33 K. Cui, Y.L. Cheng, J.M. Dai and J.P. Liu, *Mater. Chem. Phys.* 138, 2013, 810-816.
- 34 M. Ginic-Markovic, J.G. Matison, R. Cervini, G.P. Simon and P.M. Fredericks, *Chem. Mater.* 2006, 18, 6258-6265.
- 35 Y.S. Luo, D.Z. Kong, Y.L. Jia, J.S. Luo, Y. Lu, D.Y. Zhang, K.W. Qiu, C.M. Li and T. Yu, *RSC Adv.* 2013; 3: 5851-5859.
- 36 Z.X. Wei, M.X. Wan, T. Lin and L.M. Dai, *Adv. Mater.* 2003; 15: 136-139.
- 37 M. Zong, Y. Huang and N. Zhang, *Appl. Surf. Sci.* 2015; 345: 272-278.
- 38 K. Singh, A. Ohlan, V.H. Pham, R. Balasubramanian, S. Varshney, J. Jang, S.H. Hur, W.M. Choi, M. Kumar, S.K. Dhawan, B.S. Kong and J.S. Chung, *Nanoscale*, 2013; 5: 2411-2420.
- 39 J.Y. Cheng, B. Zhao, S.Y. Zheng, J.H. Yang, D.Q. Zhang and M.S. Cao, *Appl. Phys. A* 2015; 119: 379-386.
- 40 D.Q. Zhang, J.Y. Cheng, X.Y. Yang, B. Zhao and M.S. Cao, *J. Mater. Sci.* 2014; 49: 7221-7230.
- 41 B. Lu, X.L. Dong, H. Huang, X.F. Zhang, X.G. Zhu, J.P. Lei and J.P. Sun, *J. Magn. Magn. Mater.* 2008; 320: 1106-1111.
- 42 Z.H. Wang, Z. Han, D.Y. Geng and Z.D. Zhang, *Chem. Phys. Lett.* 2010; 489: 187-190.
- 43 H. Wang, Y.Y. Dai, W.J. Gong, D.Y. Geng, S. Ma, D. Li, W. Liu and Z.D. Zhang, *Appl. Phys. Lett.* 2013; 102: 223113.
- 44 Z.H. Wang, L.W. Jiang, D. Li, J.J. Jiang, S. Ma, H. Wang, D.Y. Geng, J. An, J. He, W. Liu and Z.D. Zhang, *J. Appl. Phys.* 2014; 115: 17A527.
- 45 Z.W. Li and Z.H. Yang, *J. Magn. Magn. Mater.* 2015; 387: 131-138.
- 46 X.F. Zhang, X.L. Dong, H. Huang, Y.Y. Liu, W.N. Wang, X.G. Zhu, B. Lv, J.P. Lei and C.G. Lee, *Appl. Phys. Lett.* 2006; 89: 053115.
- 47 L. Wan, J.F. Zhang, Y.Q. Chen, H.R. Wang, W.B. Hu, L. Liu and Y.D. Deng, *J. Phys. D: Appl. Phys.* 2015; 48: 355302.
- 48 X.X. Wang, M.X. Yu, W. Zhang, B.Q. Zhang and L.F. Dong, *Appl. Phys. A* 2015; 118: 1053-1058.

40